Journal of Zhejiang University-SCIENCE C (Computers & Electronics)
ISSN 1869-1951 (Print); ISSN 1869-196X (Online)
www.zju.edu.cn/jzus; www.springerlink.com
E-mail: jzus@zju.edu.cn

GaAs pHEMT multi-band/multi-mode SP9T switch for quad-band GSM and UMTS handsets applications*

Xiao-ying WANG†, Wen-ting GUO, Yang-yang PENG, Wen-quan SUI†‡

(*Zhejiang California International Nanosystems Institute (ZCNI), Zhejiang University, Hangzhou 310029, China*)

†E-mail: xiaoying8581@163.com; goldenglobe99@hotmail.com

Received May 31, 2010; Revision accepted July 7, 2010; Crosschecked Feb. 28, 2011

Abstract: A multi-band/multi-mode single-pole nine-throw (SP9T) switch for GSM/UMTS (global system for mobile communications/universal mobile telecommunication system) systems is demonstrated. The switch consists of a GaAs 0.5 μm pseudomorphic high-electron mobility transistor (pHEMT) radio frequency (RF) switches module and Si complementary metal–oxide–semiconductor (COMS) digital module with an encoder and a DC boost circuit. High isolation and high linearity are achieved by a series-shunt switch structure and the DC boost circuit, respectively. The switch shows a measured insertion loss of 0.4 dB at 0.8 GHz for GSM transmit arms, 0.7 dB at 0.9 GHz and 0.9 dB at 1.8 GHz for GSM receive arms, and 0.6 dB at 1.8 GHz for UMTS arms. The switch introduces 2nd and 3rd harmonic suppression levels less than −64 dBc at 37 dBm input power. Isolations between transmit and receive terminals are more than 48 dB when one transmit arm is activated. The size of the RF switches module is 1.5 mm×1.1 mm, and the size of the digital module is 1.3 mm×0.63 mm with gold bonding wires connecting these two modules.

Key words: GSM, UMTS, Single-pole nine-throw (SP9T), pHEMT, Encoder, DC boost
doi:10.1631/jzus.C1000178 **Document code:** A **CLC number:** TN432

1 Introduction

As a foremost component connected with antennas in wireless communication systems (Guo *et al*., 2003; Ruan *et al.*, 2007), there has been a growing demand for multi-band/multi-mode radio frequency (RF) switches since cellular phone handsets should support multi-band/multi-mode radios, e.g., the global system for mobile communications (GSM), distributed control system (DCS), personal communications service (PCS), and universal mobile telecommunication system (UMTS), especially in the midst of transition from the second generation to the third generation recently. For RF and microwave switch design, PIN diode (Brogle *et al*., 2009), microelectromechanical system (MEMS) (Kim *et al.*, 2008), and field-effect transistor (FET) (in both GaAs and CMOS processes) (Gu *et al.*, 2003; 2004; Gotch *et al.*, 2004; Kohama *et al.*, 2005; Tinella *et al.*, 2006; Prikhodko *et al*., 2007; Wu *et al.*, 2007) are three commonly used technologies. However, considering cost, integration, switching speed, power consumption, and linearity, FET switches based on III–V compounds (e.g., GaAs), especially pseudomorphic high-electron mobility transistors (pHEMTs), are the most attractive choice on the wireless communication market.

There are some published studies on RF and microwave pHEMT switches, but most of them focus on a switch with fewer arms, such as the single-pole double-throw (SP2T) switch (Gu *et al.*, 2004), SP3T switch (Gu *et al.*, 2003; 2004), SP6T switch (Gotch *et al.*, 2004; Prikhodko *et al*., 2007; Wu *et al.*, 2007), and SP7T switch (Kohama *et al.*, 2005). In this paper, a single-pole nine-throw (SP9T) RF switch which supports quad-band GSM and UMTS mobile communication systems is demonstrated. Being the

‡ Corresponding author

* Project supported by the National Natural Science Foundation of China (No. 60971058) and the Natural Science Foundation of Zhejiang Province, China (No. R107481)

foremost component in the front-end architecture, linearity should be high enough to pass on the output power of the transmit amplifier. Isolation between transmit and receive terminals, as another important figure of merit, should be high enough to decrease signal leakage from the activated arms to the inactivated arms. A series-shunt switch structure and a DC boost circuit are used to improve isolation and linearity, respectively. Good simulated and measured results are achieved and shown.

2 Circuit design

A GSM/UMTS mode cellular phone system requires that the handsets should be able to transmit and receive both GSM and UMTS signals.

2.1 RF switches module

Topological schematic of the SP9T switch consists of two parts: RF switches module and digital module. The schematic of the RF switches module is shown in Fig. 1.

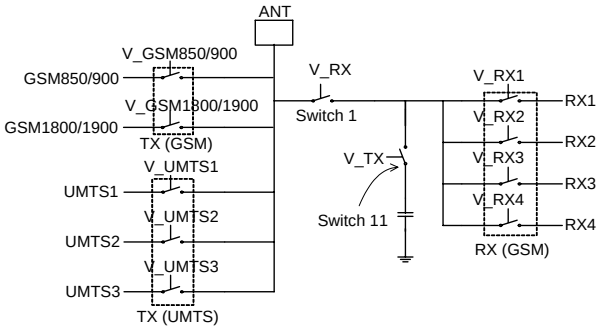

Fig. 1 Topological schematic of the RF switches module

The GSM850/900 and GSM1800/1900 are transmit arms in GSM mode, and RX1 to RX4 are corresponding GSM receive arms. UMTS1 to UMTS3 work in UMTS mode, realizing both transmit and receive functions. There are 11 controlling lines generated by a digital encoder to decide the state of each of the 11 switch units. To increase the isolation between transmit and receive terminals, a series-shunt switch 1 and switch 11 structure, which is connected with a coupling capacitor to ground, is used. When any of the TX arms detailed in Fig. 1 is activated, switch 11 is on and switch 1 is off. The RF signal leaking from 'off' switch 1 is down to ground through 'on' switch 11; therefore, the isolation between transmit and receive arms can be remarkably improved.

2.2 Digital module

A five-input eleven-output encoder and a DC boost circuit are included in the digital module. Five control lines (V_{c1}–V_{c4} and V_{dd}) are used to select one of the nine arms or an 'idle' state. The truth table for selecting each of the SP9T switch arms and 'idle' state is shown in Table 1.

Table 1 Single-pole nine-throw (SP9T) true table

Mode	V_{c1}	V_{c2}	V_{c3}	V_{c4}	V_{dd}
GSM850/900 TX	H	H	L	L	H
GSM1800/1900 TX	H	L	L	L	H
RX1	L	L	L	L	H
RX2	L	L	H	L	H
RX3	L	H	L	L	H
RX4	L	H	H	L	H
UMTS1	H	L	H	L	H
UMTS2	H	L	H	H	H
UMTS3	H	H	H	L	H
Idle	L	L	L	L	L

H: high; L: low

The function of the DC boost circuit is pulling voltage from 3 V to 7 V; thus, the control voltage of RF switches is 7 V. The high control voltage plays a tremendous part in improving linearity, which will be explained in the following section. A Dickson structure is adopted in the DC boost circuit (Fig. 2).

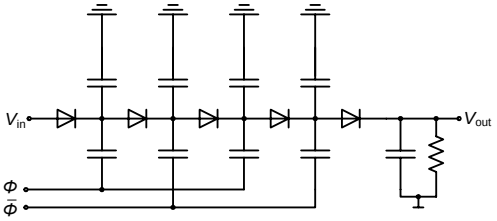

Fig. 2 DC boost circuit with a Dickson structure

2.3 Switch layout

Depletion mode 0.5 μm GaAs pHEMT is used for the RF switches module, while a 0.18 μm Si CMOS process is adopted for the digital module to minimize both size and cost. Figs. 3a and 3b show the layout and microphotograph of the RF switches module respectively, Fig. 4 shows the layout of the digital module, and Fig. 5 shows the photograph of the test board. The size of the RF switches module is

1.5 mm×1.1 mm and the size of the digital module is 1.3 mm×0.63 mm. Gold bonding wires are used to connect these two modules.

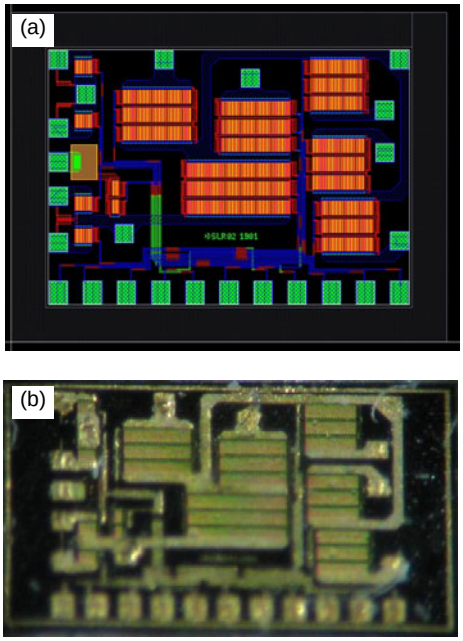

Fig. 3 Layout (a) and microphotograph (b) of the RF switches module with a size of 1.5 mm×1.1 mm

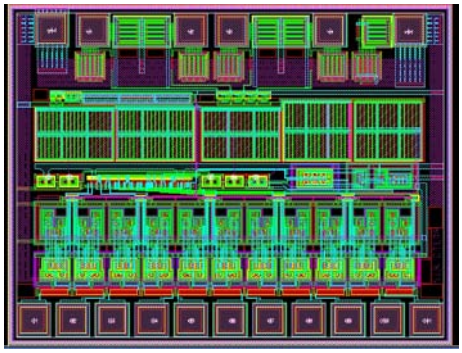

Fig. 4 Layout of the digital module with a size of 1.3 mm×0.63 mm

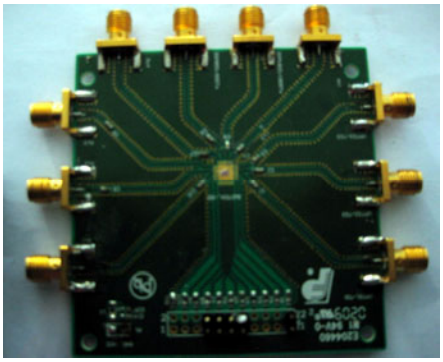

Fig. 5 Photograph of the test board

3 Switch performance

3.1 Control bias methods

There are two control bias methods for pHEMT switches in wireless, non-reference control bias and reference control bias.

For the former one, V_C is positive for the gate of the 'on' state switch arm, and other control lines are at 0 V. At least one switch arm must be in the 'on' state. For the latter, V_C is negative for all gates of 'off' state switch arms, and the 'on' state gate control is at 0 V. All RF lines are at 0 V DC. The non-reference control bias method used in this work is the most popular because of the easy realization.

3.2 Power handling capability

Take the single-pole double-throw (SPDT) switch as an example. The power handling capability of the RF switch is determined by two aspects: the largest power that the 'on' state switch arm can withstand, and the characteristic of the 'off' switch arm.

For the 'on' state switch arm, the largest power is limited by the size of the FET; thus, it can be increased as the size increases. The equation is given by

$$P_{max} = I_{DDS}^2 Z_L / 2, \quad (1)$$

where I_{DDS} is the saturation current of the FET, and Z_L is the load impedance.

For the 'off' state switch arm, FET is equivalent to a reverse-biased diode. Fig. 6 explains how it limits the power handling capability.

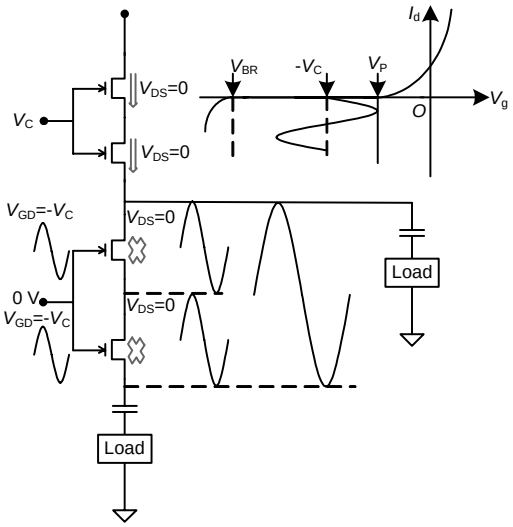

Fig. 6 Single-pole double-throw (SP2T) switch

In Fig. 6, V_C is the 'on' state control voltage, which is fixed by the DC boost circuit, and V_P is the pinch-off voltage. The voltage dropped across the gate resistance is ignored for clarity. The largest power can be obtained by

$$P_{max}=\frac{2[N(V_C+V_P)]^2}{Z_0}, \quad (2)$$

where N is the series number of the 'off' state switch arms, and Z_0 is the characteristic impedance. With series FETs, power handling capability can be greatly enhanced.

3.3 Linearity

There are two typical waveform distortions, waveform clipping and waveform asymmetry, which result in poor linearity in a switch circuit (Gu *et al*., 2004).

Waveform clipping is a large signal related distortion, mostly caused by 'off' switch arms. As can be seen from Fig. 7, RF signal is superpositioned on V_C and swings across the gate-to-drain or gate-to-source junction on both 'on' and 'off' arms. When the difference between the input RF signal voltage and gate voltage becomes larger than V_P, the output waveform is clipped. Therefore, the 'off' switch arms, which should be off through a whole RF signal cycle, would be on in a certain amount of periods.

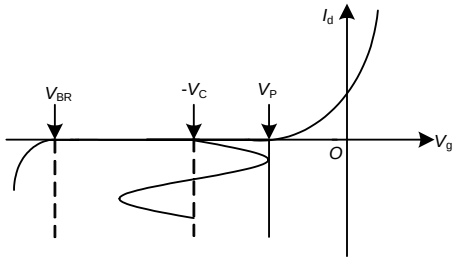

Fig. 7 Waveform clipping

There are three solutions to improve the nonlinearity caused by waveform clipping. One is to use multi-gate FETs or series FETs, which can reduce the amount of voltage dropped across the gate-to-drain or gate-to-source junctions, but this will increase the layout size. Another solution is to increase the pinch-off voltage V_P, but this will increase the on-resistance, which results in higher insertion loss, and weakens the power handling capability of the 'on' state switch arm. The most effective solution is to increase the 'on' state control voltage V_C. Thus, the 'off' switch arm can handle larger RF signal swings and deepen the 'off' level. The effectiveness can be seen from simulation results in Fig. 8.

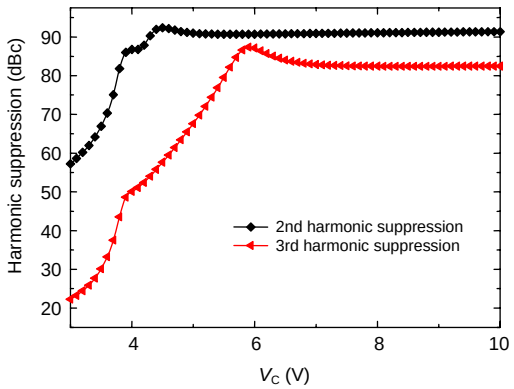

Fig. 8 Harmonic suppression as 'on' state control voltage increases (P_{in}=35 dBm, frequency=0.9 GHz)

As the 'on' state control voltage increases, the 2nd and 3rd harmonic suppressions are improved remarkably. They reach saturation when the 'on' state control voltage is high enough.

Another cause of waveform distortions is waveform asymmetry, which is generated by either small or large RF signals. For the sinusoidal RF signal waveform, it can be seen from Fig. 7 that the distortion does not exist during the negative cycle because of a more completely shut off channel in the 'off' state switch arms when the RF signal level increases. During the positive cycle, however, the channel is less shut off due to a more positive level, resulting in a smaller signal current in the positive cycle than normal current in the negative cycle. Thus, a signal asymmetry distortion occurs and there is no effective method to avoid this asymmetry.

4 Results and discussion

In the RF switches module, arm GSM850/900 and arm GSM1800/1900 are identical, the three arms in UMTS mode are identical in schematic, and the four receive arms are identical. Thus, only simulated and measured results of arms GSM850/900, UMTS1, and RX1 are plotted.

Fig. 9 is the simulated and measured insertion losses (ILs) of arms GSM850/900, UMTS1, and RX1. The measured IL results include the loss of the PCB board, which is approximately 0.3 dB at 0.9 GHz and 0.43 dB at 1.8 GHz. Metal lines in the layout cause measured IL to be greater than simulated IL. According to the measured IL results (Fig. 9), we can calculate that IL at 0.8 GHz of the GSM arm is about 0.4 dB, IL at 1.8 GHz of the UMTS arm is about 0.6 dB, and ILs at 0.9 GHz and 1.8 GHz of the RX arm are about 0.7 dB and 0.9 dB, respectively. IL values are acceptable in the GSM/UMTS system.

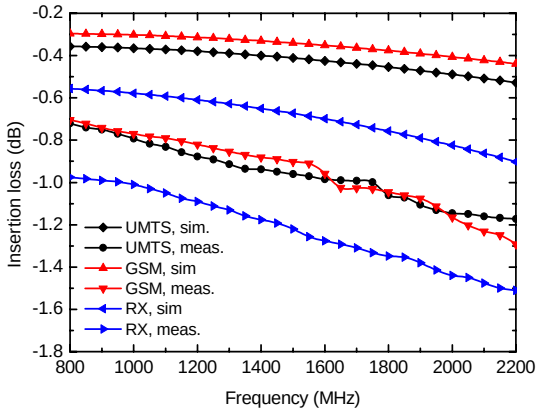

Fig. 9 Simulated (sim.) and measured (meas.) insertion losses of arms GSM850/900, UMTS1, and RX1

Fig. 10 is the simulated and measured isolations between transmit and receive terminals as one of the SP9T switch arms is activated. GSM-RX isolation and UMTS-RX isolation are remarkably high as the GSM arm and UMTS arm are at 'on' state, respectively. They are more than 48 dB when one transmit arm is activated, as can be seen from Figs. 10a and 10b. The series-shunt switch structure is playing a significant role here.

Fig. 11 is the simulated and measured harmonic suppressions of arms GSM850/900, GSM1800/1900, and UMTS1. Harmonics cannot be read from the Agilent PSA series spectrum analyzer since the 2nd and 3rd harmonics are submerged beneath the noise when input power is low. As the GaAs pHEMT model provided by the foundry is inaccurate in the high input power and high frequency condition, the measured 2nd and 3rd harmonic suppressions are very different from simulated ones. Harmonic suppressions drop quickly as input power rises. It is difficult to obtain high harmonic suppressions at high input power. In this design, 2nd and 3rd harmonic suppressions of arms GSM850/900 and GSM1800/1900 are all below −64 dBc until 37 dBm input power, and 2nd and 3rd harmonic suppressions of arm UMTS1 at different frequency points are all below −70 dBc until 32 dBm input power.

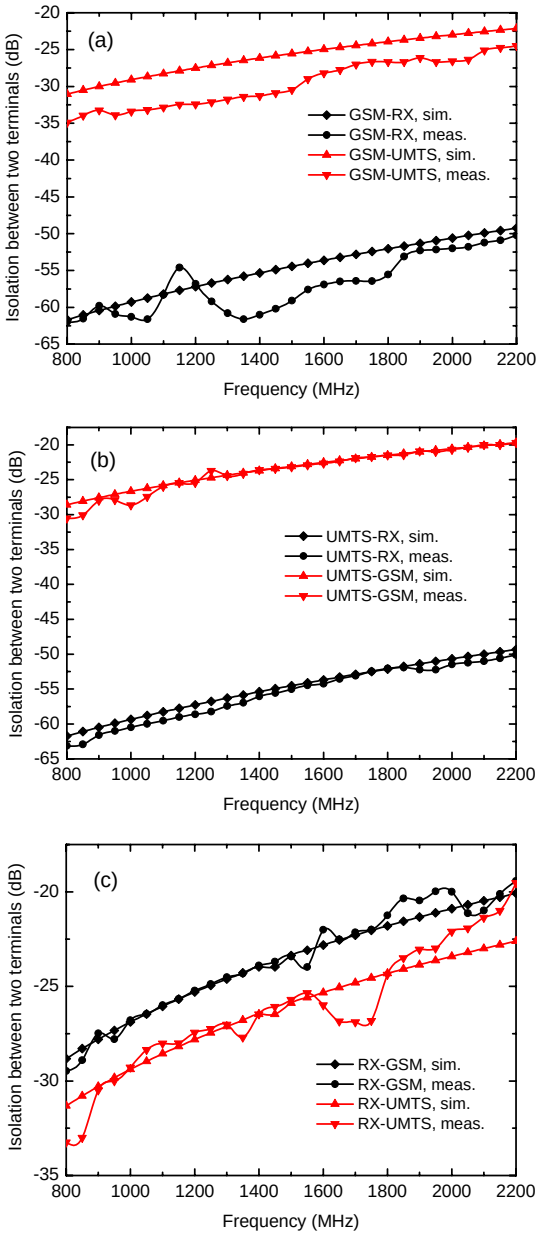

Fig. 10 Simulated (sim.) and measured (meas.) isolations between transmit and receive terminals as one of the single-pole nine-throw (SP9T) switch arms is activated
(a) Arm GSM850/900 on; (b) Arm UMTS1 on; (c) Arm RX1 on

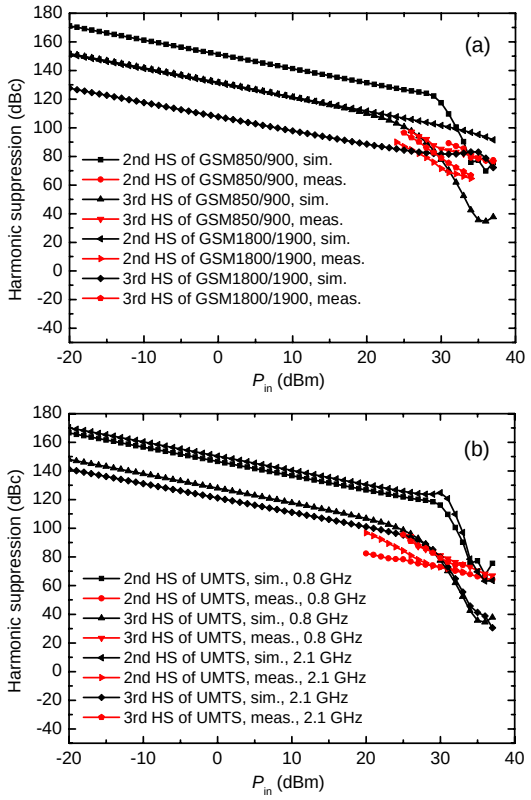

Fig. 11 Simulated (sim.) and measured (meas.) harmonic suppressions for arms GSM850/900 and GSM1800/1900 (a) and arm UMTS1 at 2.1 GHz and 0.8 GHz (b)

5 Conclusions

The design of the SP9T switch with an encoder and a DC boost circuit for a quad-band GSM/UMTS mobile communication system has been discussed in detail. Isolations between transmit and receive terminals and linearity are remarkably improved by a series-shunt switch structure and a DC boost circuit, respectively. The switch shows an insertion loss of 0.4 dB at 0.8 GHz for GSM arms, 0.6 dB at 1.8 GHz for UMTS arms, and 0.7 dB at 0.9 GHz and 0.9 dB at 1.8 GHz for RX arms. The 2nd and 3rd harmonic suppression levels of arms GSM850/900 and GSM1800/1900 are below −64 dBc until 37 dBm input power, and below −70 dBc until 32 dBm input power for UMTS arms. The isolations between transmit and receive terminals are more than 48 dB when one transmit arm is activated. The size of the RF switches module is 1.5 mm×1.1 mm and the size of the digital module is 1.3 mm×0.63 mm with gold bonding wires connecting these two modules.

References

Brogle, J.J., Curcio, D.G., Hoag, D.R., Boles, T.E., 2009. Multithrow Heterojunction PIN Diode Switches. European Microwave Integrated Circuits Conf., p.9-12.

Gotch, D., Goh, T., Jackson, R., 2004. State-of-the-Art Low Loss, High Isolation SP6T Switch for Handset Application. 7th European Conf. on Wireless Technology, p.17-20.

Gu, Z., Johnson, D., Belletete, S., Frykund, D., 2003. A 2.3 V PHIEMT Power SP3T Antenna Switch IC for GSM Handsets. IEEE 25th Annual Technical Digest Gallium Arsenide Integrated Circuit (GaAs IC) Symp., p.48-51.

Gu, Z., Johnson, D., Belletete, S., Fryklund, D., 2004. Low Insertion Loss and High Linearity PHEMT SPDT and SP3T Switch ICs for WAN 802.11 a/b/g Applications. IEEE Radio Frequency Integrated Circuits Symp., p.505-508. [doi:10.1109/RFIC.2004.1320667]

Guo, Y.X., Chia, M.Y.W., Chen, Z.N., 2003. Compact Multi-band Antennas for Wireless Communications. Progress in Electromagnetics Research Symp., p.130.

Kim, J.M., Lee, S., Baek, C.W., Kwon, Y., Kim, Y.K., 2008. BCB-based wafer-level packaged single-crystal silicon multi-port RF MEMS switch. *Electron. Lett.*, **44**(2):118-119. [doi:10.1049/el:20083288]

Kohama, K., Nakamura, M., Onodera, K., Wada, S., Tamari, S., Mizunuma, Y., 2005. An Antenna Switch MMIC for GSMKJMTS Handsets Using E/D-Mode JPHEMT Technology. IEEE Radio Frequency Integrated Circuits Symp., p.509-512. [doi:10.1109/RFIC.2005.1489859]

Prikhodko, D., Tkachenko, Y., Sprinkle, S., Carter, R., Nabokin, S., Chiesa, J., 2007. Design of a Low VSWR Harmonics, Low Loss SP6T Switch for GSM/Edge Applications. Proc. 2nd European Microwave Integrated Circuits Conf., p.32-35. [doi:10.1109/EMICC.2007.4412640]

Ruan, Y.F., Guo, Y.X., Khoo, K.W., Shi, X.Q., 2007. Compact wideband antennas for wireless communications. *IET Microwave Antenn. Propag.*, **1**(3):556-560. [doi:10.1049/iet-map:20060245]

Tinella, C., Richard, O., Cathelin, A., Réauté, F., Majcherczak, S., Blanchet, F., Belot, D., 2006. 0.13 μm CMOS SOI SP6T Antenna Switch for Multi-standard Handsets. Topical Meeting on Silicon Monolithic Integrated Circuits in RF Systems, p.58-61. [doi:10.1109/SMIC.2005.1587904]

Wu, J.W., Chen, S.W., Huang, C.C., Tang, C.W., Li, J.H., Tsai, C.W., 2007. PHEMT SP6T ICs for Quadband GSM Handset Applications. Proc. Asia-Pacific Microwave Conf., p.1-4. [doi:10.1109/APMC.2007.4554719]